### Title

A membrane-activatable near-infrared fluorescent probe with ultra-photostability for mitochondrial membrane potentials.




### Journal

The Analyst, 141(12)

### ISSN

0003-2654



### Authors

Ren, Wei
Ji, Ao
Karmach, Omran
et al.



### Publication Date

2016-06-01

### DOI

10.1039/c5an01860a

Peer reviewed

Analyst

PAPER

View Article Online
View Journal | View Issue



Cite this: *Analyst*, 2016, **141**, 3679

# A membrane-activatable near-infrared fluorescent probe with ultra-photostability for mitochondrial membrane potentials†

Wei Ren,‡[a] Ao Ji,‡[a] Omran Karmach,[b] David G. Carter,[c] Manuela M. Martins-Green*[b] and Hui-wang Ai*[a]

Received 9th September 2015,
Accepted 28th October 2015

DOI: 10.1039/c5an01860a

www.rsc.org/analyst

Mitochondrial membrane potential (MMP) is a frequently used indicator for mitochondrial function. Herein, we report a photostable near-infrared (NIR) fluorescent dye for monitoring MMP. This new probe, named NIMAP, is non-fluorescent in aqueous solution and can be activated by cell membranes, providing high fluorescence contrast and low background fluorescence. NIMAP has been validated for monitoring MMP in living mammalian cells and in mice. Due to the large fluorescence response, low fluorescence background, high photostability, and excellent tissue penetration resulting from red-shifted excitation and emission in the "optical window" above 600 nm, broad applications of this new probe are expected.

## Introduction

Mitochondrial membrane potential (MMP) is required for cellular respiration and ATP synthesis.[1] It is also important for intracellular calcium dynamics, the production of reactive oxygen species, neural synapse, inflammation, cell proliferation, and cell death.[2–6] A direct monitoring of MMP is, therefore, of high interest. Previously, tetraphenylphosphonium ($TPP^+$)-sensitive microelectrodes have been used to measure the membrane potentials of isolated mitochondria or mitochondria in permeabilized cells.[7] Measuring absolute MMP in living cells is technically challenging.[8] There are only few reports, which used end-point measurements based on radioisotope tracers to assay absolute MMP in suspensions of living cells.[9,10] On the other hand, fluorescent MMP sensors are popular for assessing MMP in living cells,[11] despite that only qualitative or semi-quantitative information can typically be derived from those imaging experiments. Fluorescent MMP dyes are mostly lipophilic cationic compounds. When applied to healthy cells, they tend to accumulate in the inner mitochondrial inner membrane, because healthy cells maintain cytoplasmic and mitochondrial transmembrane potentials to induce a negatively charged mitochondrial inner membrane.[12] The distribution of these probes is affected by the transmembrane electric fields, following the Nernst equation.[13] Therefore, the observed mitochondrial fluorescence intensity can be utilized as an indicator for MMP, although other factors, such as the cytoplasmic transmembrane potential, the volume ratio of the mitochondria and a whole cell, and the participation coefficients of dyes in mitochondria and the cytosol, also have an impact on the mitochondrial accumulation of these cationic molecules.

Fluorescent probes with excitation and emission in the 600–900 nm spectral region are desirable for mammalian studies, due to the weak absorbance of hemoglobin, myoglobin, melanin, and water in this NIR optical window.[14,15] Moreover, compared to light at shorter wavelengths, light with wavelengths matching this optical window overlaps less with the excitation of endogenous chromophores, such as flavins and NADH.[16] These lower-energy photons also cause less photodamage to living cells and tissues.[17] Not surprisingly, a current trend is to develop novel fluorescent dyes and sensors that fluoresce in this NIR spectral region, such as recently reported NIR dyes that are sensitive to cytoplasmic membrane potentials or that can highlight the mitochondrial structure in live cells.[18,19] Common MMP dyes,[11] such as TMRM (tetramethylrhodamine methyl ester), TMRE (tetramethylrhodamine ethyl ester), Rhodamine 123, and JC-1, and a recent TPE-indo dye[20] all have fluorescence excitation and emission peaks less than 600 nm. Other concerns of these existing MMP probes include nonspecific background fluorescence, poor localization, high cytotoxicity, and unsatisfactory photostability.[11]

[a]*Department of Chemistry, University of California, Riverside, CA 92521, USA. E-mail: huiwang.ai@ucr.edu*
[b]*Department of Cell Biology and Neuroscience, University of California, Riverside, CA 92521, USA. E-mail: manuela.martins@ucr.edu*
[c]*Institute for Integrative Genome Biology, University of California, Riverside, CA 92521, USA*

† Electronic supplementary information (ESI) available: Procedures for chemical synthesis, spectroscopic characterization, experimental optimization and comparison, and time-lapse movies. See DOI: 10.1039/c5an01860a

‡ These two authors contributed equally to this work.

Herein, we report the development of a NIR probe (designated NIMAP) for monitoring MMP in living mammalian cells and mice. NIMAP is highly attractive, because not only does it command the above-mentioned advantages of a NIR probe, but it also shows a large fluorescence response to MMP changes, membrane-activated fluorescence and minimal background signals, ultra-photostability, and excellent tissue penetration in live animals.

# Experimental

### Materials and general methods

All chemicals and reagents were purchased from Fisher Scientific (Pittsburgh, PA) or Sigma-Aldrich (St. Louis, Mo) unless specified elsewhere. Plasmid DNA was purified using Syd Laboratories Miniprep columns (Malden, MA). The scheme and procedure to synthesize NIMAP are outlined in the ESI.† The structure and purity of NIMAP were analyzed with ESI-MS, $^{1}$H NMR, and $^{13}$C NMR. ESI-MS was run on an Agilent LC-TOF system by direct fusion. NMR spectra were recorded on a Varian Inova 400 instrument with chemical shifts relative to tetramethylsilane. Stock solutions of NIMAP were made in DMSO (Sigma-Aldrich).

### Spectroscopic characterization

A monochromator-based Synergy Mx Microplate Reader (BioTek, Winooski, VT) was used to record all spectra. The absorption spectrum of NIMAP was measured by preparing NIMAP (50 μM) in a 1 : 1 (v/v) mixture of methanol and Tris-HCl aqueous buffer (50 mM, pH 7.4). Absorbance values of NIMAP at 600 nm was measured at various pH conditions by preparing a series of 1 : 1 (v/v) mixtures of methanol and aqueous solutions containing citric acid (200 mM) and phosphate (200 mM) with a pH range from 3 to 11. To measure the fluorescence excitation and emission spectra of NIMAP, we prepared NIMAP in liposomes as described elswhere.[21] L-α-Lecithin egg yolk and cholesterol were purchased from EMD Millipore (Billerica, MA) and Alfa Aesar (Ward Hill, MA), respectively. Cholesterol (2.5 mg) and L-α-Lecithin egg yolk (10 mg) in chloroform : methanol (v/v 3 : 2) were vacuumed on a rotary evaporator for 3 h to form a thin, oily film on the glass wall of the flask. Next, double distilled water (dd$H_2O$, 1 mL) was added and the rotation of the rotary evaporator continued for another 15 min to form an oil/water mixture in the flask. The resulting mixture was then sonicated 5 min on a probe sonicator to yield a slightly hazy and transparent solution. Formed liposomes were next diluted with equal volume phosphate buffered saline (PBS, pH 7.4). NIMAP was added to a final concentration of 100 μM. The mixture was incubated at room temperature for 15 min. To record the emission spectrum, the excitation wavelength was set at 630 nm, and the emission scanned from 650 nm to 870 nm. To record the excitation spectrum, the emission wavelength was set at 730 nm, and the excitation scanned from 500 nm to 700 nm. To determine the responsiveness of NIMAP fluorescence to pH changes, we mixed NIMAP (50 μM) with a series of 9 : 1 (v/v) mixtures of glycerol and the aforementioned aqueous solutions with a pH range from 3 to 11. Fluorescence at 710 nm was recorded with the excitation wavelength set at 650 nm.

### Mammalian cell culture and dye loading

Human embryonic kidney (HEK) 293T cells or cervical cancer HeLa cells were maintained in T25 flasks containing 5 mL Dulbecco's Modified Eagle's Medium (DMEM) supplemented with 10% fetal bovine serum (FBS) and incubated at 37 °C with 5% CO2 in humidified air. Cells at 80% confluence were passaged into 35 mm culture dishes in a ratio of 1 : 5 or 1 : 20 for transfection or direct dye loading on the following day. To stain cells, fluorescent dyes were added into the cell culture medium, and the incubation condition was typically 45 min at 37 °C, unless stated otherwise.

### Mammalian cell transfection

Transfection complexes were prepared by mixing DNA and PEI (polyethylenimine, linear, 25 kD; DNA : PEI [w/w] = 1 : 2.5) in Opti-MEM at room temperature for 20 min. For every 35 mm culture dish, 10 μL PEI (1 μg μL$^{-1}$) was used to prepare a 500 μL transfection mixture. We used a pcDNA3 plasmid harboring a mitochondria-localized mWasabi (Mito-mWasabi).[22] The prepared transfection mixture was then added to cells and incubated for 2 h at 37 °C. Next, pre-warmed, fresh DMEM containing 10% FBS was used to replace the transfection medium. On the following day, cells were stained with NIMAP before imaging.

### Fluorescence imaging

Fluorescence microscopy was performed with a Leica SP5 inverted confocal fluorescence microscope with the spectral imaging capability (Leica, Boston, MA), unless otherwise stated. The instrument was equipped with a 488 nm laser (1.5 mW at full power), a 514 nm laser (2 mW at full power), and a 633 nm laser (1 mW at full power). A 40× water lens was used for all imaging studies. Unless otherwise noted, NIMAP was imaged using a 633 nm laser line at 15% laser power for excitation, and the gain was set to 800 mV. The emission was set from 650 nm to 800 nm. To record the emission spectrum for NIMAP loaded into live-cell mitochondria, the emission bandwidth was set at 10 nm and images were taken from 650 nm to 790 nm. To image mWasabi GFP, the excitation was set at 488 nm with 10% laser power, and the gain was set to 900 mV. The emission channel was set from 495 nm to 550 nm. To image Rhodamine 123, the excitation was set at 514 nm with 15% laser power, and the gain was set to 900 mV. The emission was set from 525 nm to 570 nm. Time-lapse images were acquired every minute. After the initial few frames, oligomycin (MP Biomedicals, Solon, OH) was added to a final concentration of 1 μg mL$^{-1}$. Several additional consecutive images were acquired before adding FCCP (Enzo Life Sciences, Farmingdale, NY) at a final concentration of 100 nM. Additional frames were recorded. Similarly, we added $H_2O_2$ (0.2%) to fresh HEK 293T cells loaded with NIMAP. Images

 

were captured at 1 min intervals to observe the changes in mitochondrial membrane potential and morphology. Cell images were processed with Leica Application Suite (LAS) or ImageJ.

### Mouse imaging

Human prostate cancer PC3 cells were cultured as previously described.[23] At 100% confluency, $4 \times 10^6$ cells per group were stained with NIMAP (10 μM) or Rhodamine 123 (10 μM) for 1 h at 37 °C. After staining with NIMAP, cells were washed once with 5 ml of PBS. For collection, cells were suspended in the culture medium and centrifuged at 3000 rpm for 2 min. Cells were then resuspended in PBS and centrifuged at 3000 rpm for 2 min. The staining of cells with Rhodamine 123 was similar, except two additional washes were carried out prior to the collection of cells in order to remove excess Rhodamine 123. Briefly, cells were allowed to incubate with the fresh culture medium at 37 °C for 1 h, and this process was repeated before collection of cells. Next, $4 \times 10^6$ cells were resuspended in 100 μL PBS and injected subcutaneously into the back of immunocompromised NOD *scid* gamma mice (Jackson Laboratory, Stock # 005557) after air removal. Mice were imaged several times over a week, using a Luminescence Dark Box equipped with light-emitting diodes (LED) for excitation. To record the fluorescence of NIMAP, we used a 630 nm LED array, a 650/40 nm bandpass excitation filter, and a 695/30 nm bandpass emission filter. To record the fluorescence of Rhodamine 123, we used a 490 nm LED array, a 500/40 nm bandpass excitation filter, and a 550/30 nm bandpass emission filter. Images were processed with ImageJ.

## Results and discussion

### Designing and preparation of NIMAP

Our development of the new NIR MMP probes originated from a Förster resonance energy transfer (FRET) experiment in our laboratory, which used a QSY-21 core structure as a dark quencher.[24] QSY-21 (**1** in Fig. 1) is essentially nonfluorescent (zero quantum yield) and has a high extinction coefficient (90 000 $M^{-1}$ $cm^{-1}$ at 661 nm).[25] It has been widely utilized as an efficient nonfluorescent FRET acceptor for far-red and NIR fluorophores. We prepared a QSY-21 labeled biotin derivative (**2**), and observed mitochondria-like organellar fluorescence in cultured mammalian cells stained with 100 μM of the dye (ESI Fig. S1A†). In contrast, incubating HEK 293T cells with a neutral zwitterionic sulfonic acid form of QSY-21 (**3**) did not induce significant NIR mitochondrial fluorescence (Fig. S1B†). Unstained HEK 293T cells also had no autofluorescence at this spectral region (Fig. S1C and S1D†). Considering the facts that QSY-21 labeled biotin has some degrees of lipophilicity and a positive charge, we reasoned that it was partially sequestered into the lipid bilayers of cells, followed by migration into mitochondria and fluorescence activation in this hydrophobic, viscous microenvironment.

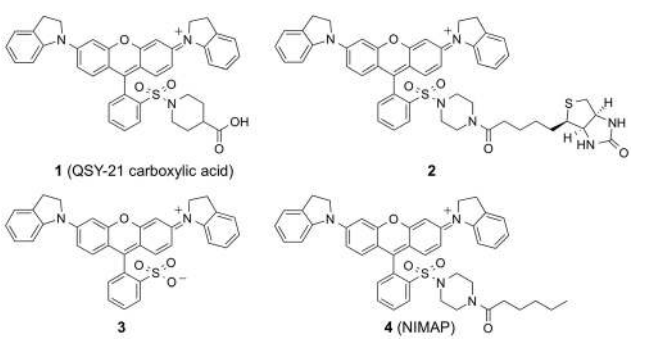


Fig. 1 Chemical structures of the dark quencher QSY-21 (**1**), a QSY-21 labeled biotin (**2**), a sulfonic acid form of QSY-21 (**3**), and NIMAP (**4**).

In light of the potential use of QSY-21 derivatives as mitochondrial dyes, we designed a new molecule (**4**) containing a hexanoamide connected to the QSY-21 core through a piperazine sulfonamide linker. A short C6 fatty acid chain was chosen to enhance the lipophilicity while retaining adequate solubility of the resultant molecule in neutral aqueous solutions for dye loading. This molecule was designated "NIMAP" for its *NI*R, *m*itochondria-*a*ctivatable *p*roperty. A synthetic route was developed to prepare NIMAP in 7 steps with 18% overall yield from commercially available, inexpensive starting materials (ESI Scheme S1†).

### Optimization of NIMAP loading into mammalian cells

We next loaded various concentrations of NIMAP into HEK 293T cells. No obvious cell death was observed upon 24 h incubation with up to 100 μM NIMAP. We also studied the impacts of dye concentrations and loading time on the accumulation of NIMAP in mitochondria at 37 °C. To keep the loading period as short as 45 min, 1–5 μM NIMAP in the cell culture medium was needed to induce strong mitochondrial fluorescence detectable by confocal microscopy with reasonable instrumental settings (Fig. S2A†). In comparison, 100 μM **2** was needed to gain similar images (Fig. S1A†). These results indicate that the fusion of the QSY-21 core with a C6 fatty acid chain increases its partition into the lipid phase and its accumulation in mammalian mitochondria.

The length of the loading period also affected the localization of NIMAP. With 1 μM NIMAP, the mitochondrial fluorescence continuously increased in a 2 h test window (Fig. S2B†), indicating that an equilibrium state for dye distribution was not reached under these conditions. At 2 h, NIMAP started to saturate mitochondria to also stain cytoplasmic membrane (Fig. S2C†). Due to the common practice favoring short loading time, we used 1 μM NIMAP and a 45 min dye incubation time in most of our following cell studies. No wash step was needed to remove excess NIMAP in these experiments because NIMAP was nonfluorescent in aqueous solutions. By comparison, the background fluorescence of HEK 293T cells stained with a conventional MMP dye, Rhodamine 123, was strong before washing off excess dye molecules (Fig. S3†). We also noticed a drastic difference of NIMAP and Rhodamine 123 in terms of their photostability (Fig. 2). Almost no photo-

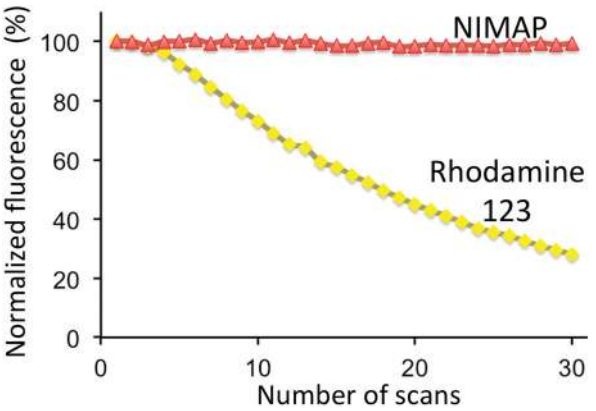


Fig. 2 Photostability of NIMAP (red) and rhodamine 123 (yellow) in HEK 293T cells under a confocal microscope.

bleaching was observed for NIMAP under the highest laser power (100% of 1 mW at 633 nm), whereas Rhodamine 123-stained cells photobleached quickly under a similar condition (50% of 2 mW at 514 nm). The excellent photostability of NIMAP makes it suitable for long-term time-lapse imaging.

### Mitochondrial localization of NIMAP

To further confirm the mitochondrial localization of NIMAP, we loaded the molecule into HEK 293T cells simultaneously expressing a green fluorescent mWasabi protein fused to a mitochondrial localization tag (Mito-mWasabi).[22] Dual colour imaging verified the colocalization of mWasabi and NIMAP in the mitochondria (Fig. 3). The ability to use NIMAP and a green fluorescent probe for dual color imaging is important because many existing, popular fluorescent sensors are based on GFP, whereas the fluorescence excitation or emission of common MMP probes, such as Rhodamine 123 and JC-1,[11] is partially overlapped with that of GFP.

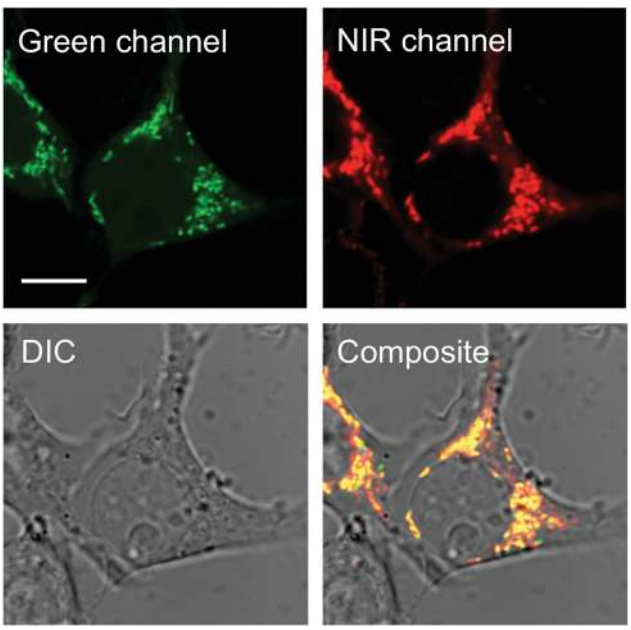


Fig. 3 Colocalization of mitochondrial mWasabi (green channel) and NIMAP (NIR channel) in HEK 293T cells (scale bar: 30 μm).

### Fluorescence activation of NIMAP by biolipids

To determine whether the observed mitochondrial fluorescence was due to the activation of NIMAP by the lipid membrane, we prepared NIMAP-containing liposomes, following a previously reported liposome-synthetic procedure.[21] The fluorescence of NIMAP-containing liposomes was high (Fig. 4). The excitation maximum is 650 nm and the emission maximum is 710 nm. In comparison, NIMAP alone was essentially non-fluorescent in aqueous solutions. Moreover, the emission profile of NIMAP in liposomes was similar to that of NIMAP in live-cell mitochondria (Fig. S4A†). A previous molecular dynamics (MD) study suggests that QSY-21 fluorescence is quenched by ring rotations and electron transfer in the excited state.[26] It is possible that the packed, viscous lipid microenvironment may restrict the rotations and electron transfer of NIMAP to enhance its fluorescence. We also measured the absorbance of NIMAP in an aqueous solution, which was similar to the profile of NIMAP fluorescence excitation in liposomes (Fig. 4). Moreover, the absorbance was insensitive to pH changes from pH 4 to 10 (Fig. S4B†). We further characterized the *in vitro* fluorescence of NIMAP in a series of aqueous buffers containing 90% (v/v) glycerol, and the fluorescence intensities were essentially unchanged from pH 4 to 10. These results are aligned with the conventional use of QSY-21 as a dark quencher and our new finding that the fluorescence of QSY-21 is greatly enhanced upon being integrated into the mitochondrial membrane.

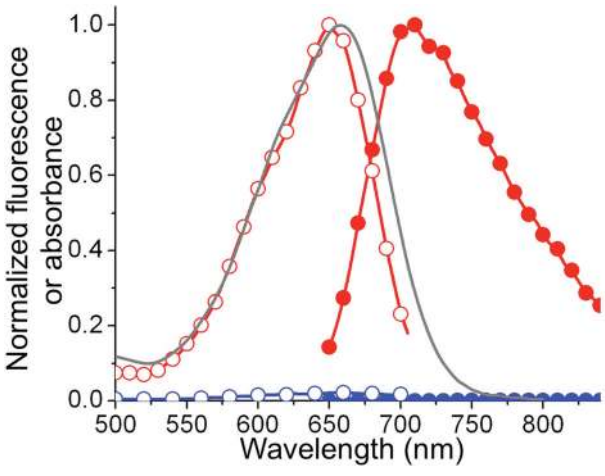


Fig. 4 Fluorescence excitation (open circle) and emission (closed circle) spectra of NIMAP in liposomes (red) or an aqueous solution (blue). The normalized absorbance of NIMAP in the aqueous solution is also shown (gray line).

### Validation of NIMAP for monitoring MMP in HEK 293T cells

Fluorescent dyes that can highlight mitochondrial structures are not necessarily sensors for MMP. For example, MitoTracker dyes and TPE-TPP probes are unresponsive to MMP changes, despite their proper mitochondrial localization.[27,28] To determine whether the fluorescence of NIMAP is responsive to MMP changes, HeLa cells were loaded with NIMAP (1 μM) and stimulated with oligomycin (1 μg $mL^{-1}$), an oxidative phosphorylation inhibitor. Due to the role of oligomycin in inhibiting ATP synthase,[29] the fluorescence of NIMAP-labeled mitochondria increased slowly, indicating a gradual increase of MMP (Fig. 5). Next, we treated the cells with carbonilcyanide *p*-triflouromethoxyphenylhydrazone (FCCP, 100 nM), a mitochondrial uncoupler. FCCP is expected to increase the ionic permeability of mitochondrial membrane, and therefore, dissipate MMP.[30] As expected, a sharp diminishment of mitochondrial fluorescence was observed (Fig. 5 and Movie S1†). This experiment validated the capability of NIMAP as an effective MMP probe, because oligomycin and FCCP are both standard chemicals known to induce MMP changes in living cell.[11]

Furthermore, we used NIMAP to monitor MMP in living cells treated with hydrogen peroxide ($H_2O_2$, 0.2‰), a strong oxidizing agent that can cause mitochondrial dysfunction and cell apoptosis.[31] When NIMAP-loaded HEK 293T cells were incubated with $H_2O_2$, mitochondrial fluorescence largely diminished in less than 10 min after addition of $H_2O_2$, indicating an oxidation-induced disruption of MMP (Fig. 6A, B, and Movie S2†). The morphology of the mitochondria also changed: they were enlarged after the stimulation. We also performed an *in vitro* experiment to monitor the fluorescence of NIMAP-containing liposomes after incubation of $H_2O_2$ (0.2‰). The fluorescence was stable, suggesting that there was no direct reaction between NIMAP and $H_2O_2$ (Fig. S5†).

### Monitoring MMP with NIMAP in mice

We next explored the use of NIMAP to monitor mitochondrial function in living mammals. We subcutaneously injected

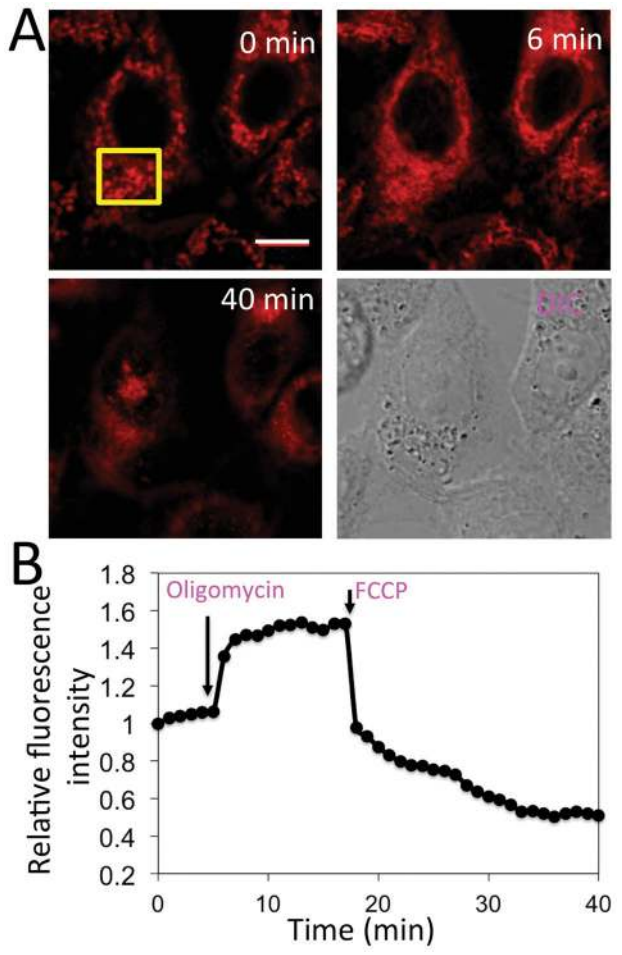


**Fig. 5** (A) Fluorescence images of NIMAP-stained HeLa cells treated with FCCP (100 nM) and oligomycin (1 μg $mL^{-1}$), at the indicated time points (Scale bar: 30 μm). (B) Time-lapse fluorescence intensities of the yellow-boxed area in panel A, normalized to the intensity at 0 min. Oligomycin and FCCP were added at 5 and 17 min, respectively.

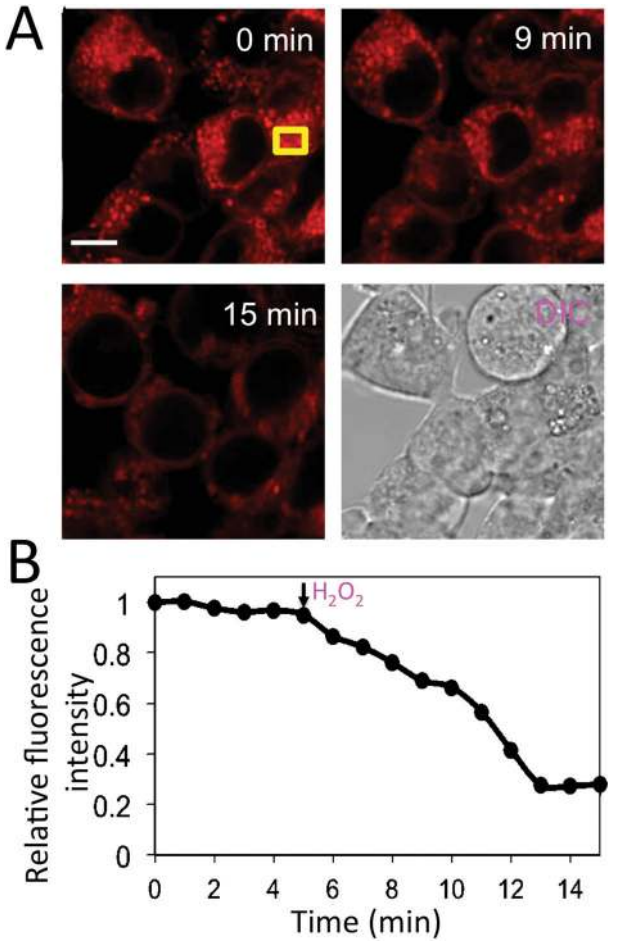


**Fig. 6** (A) Fluorescence images of NIMAP-stained HEK 293T cells treated with $H_2O_2$ (0.2‰), at the indicated time points (scale bar: 30 μm). (B) Time-lapse fluorescence intensities of the yellow-boxed area in panel A, normalized to the intensity at 0 min. $H_2O_2$ was added at 5 min.

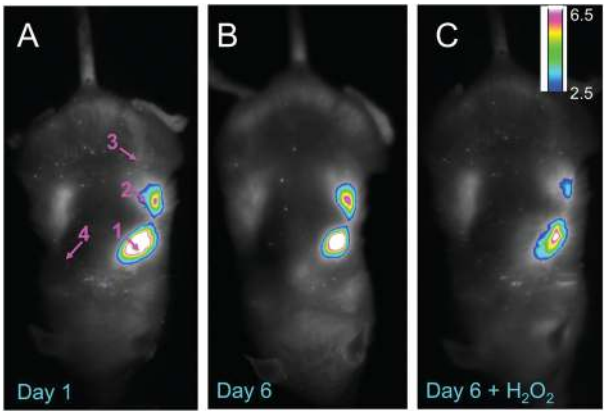


**Fig. 7** Fluorescence images of PC3 cells subcutaneously injected into euthanized mice (site 1: NIMAP-stained cells; site 2: rhodamine 123-stained cells; site 3: NIMAP-stained cells treated with $H_2O_2$ before mouse injection; and site 4: unstained cells). Sites 1 and 2 were treated with additional $H_2O_2$ in day 6.

NIMAP-stained PC3 human prostate cancer cells into a severe combined immunodeficiency (SCID) mouse and observed strong signals from these NIMAP-stained cells (Fig. 7A). For comparison, we also administered cells stained with Rhodamine 123, cells stained with NIMAP and pre-treated with $H_2O_2$, and cells without staining into SCID mice. We observed much weaker signals for Rhodamine 123-stained cells, compared to NIMAP-stained cells; and almost no signal for the other two groups. We want to note that, before injection, additional wash steps were carried out to remove excess Rhodamine 123. The same procedure was not performed for NIMAP, since excess NIMAP was nonfluorescent. This unique property of NIMAP not only simplified the experiment, but also enabled the loading of high doses of NIMAP. We next monitored the mouse for a week and observed that, at day 6 after injection of the cells, the staining signals for spots 1 and 2 were still present (Fig. 7B). We then injected additional $H_2O_2$ (0.2%, 50 μL) into the mouse at the site in proximity to the NIMAP-stained cells, and observed the $H_2O_2$-induced disruption of MMP as indicated by a fluorescence decrease at 15 min post-injection (Fig. 7C). Taken together, these experiments corroborate that NIMAP is an effective fluorescent probe with the potential for monitoring MMP and mitochondrial function *in vivo*.

## Conclusions

In summary, starting from a nonfluorescent dark quencher QSY-21, we have developed a new NIR probe, NIMAP, for monitoring MMP in living mammalian cells and *in vivo*. Lipid membranes can activate the fluorescence of NIMAP, and therefore the loading procedures can be simplified to gain low fluorescence background and high fluorescence contrast. When NIMAP was loaded into the mitochondria of living mammalian cells, it responded to MMP changes induced by chemicals with high sensitivity. NIMAP is quite photostable and spectrally compatible with common green fluorescent probes for multi-color multiplex imaging. Because of its excitation and emission at wavelengths above 600 nm, excellent penetration of mouse skin tissue was also observed. With all of these favourable photobiophysical properties, NIMAP is expected to be a powerful tool for studying MMP and mitochondrial function in various biological settings. In addition, the mitochondrial localization capability of the QSY-21 scaffold may further be exploited to construct other mitochondria-targeting fluorescent probes or selectively deliver inhibitors of mitochondrial enzymes.

## Acknowledgements

This material is based upon work supported by the University of California Riverside. H. W. A. is grateful to the U.S. National Science Foundation for a CAREER award (CHE-1351933).

## Notes and references

1 L. B. Chen, *Annu. Rev. Cell Biol.*, 1988, **4**, 155–181.
2 J. Henry-Mowatt, C. Dive, J. C. Martinou and D. James, *Oncogene*, 2004, **23**, 2850–2860.
3 M. R. Duchen, *J. Physiol.*, 2000, **529**, 57–68.
4 M. P. Murphy, *Biochem. J.*, 2009, **417**, 1–13.
5 Z. B. Andrews, S. Diano and T. L. Horvath, *Nat. Rev. Neurosci.*, 2005, **6**, 829–840.
6 B. G. Heerdt, M. A. Houston, A. J. Wilson and L. H. Augenlicht, *Cancer Res.*, 2003, **63**, 6311–6319.
7 T. S. Lim, A. Davila, D. C. Wallace and P. Burke, *Lab Chip*, 2010, **10**, 1683–1688.
8 M. D. Brand and D. G. Nicholls, *Biochem. J.*, 2011, **435**, 297–312.
9 A. A. Gerencser, C. Chinopoulos, M. J. Birket, M. Jastroch, C. Vitelli, D. G. Nicholls and M. D. Brand, *J. Physiol.*, 2012, **590**, 2845–2871.
10 S. Krauss, C. Y. Zhang and B. B. Lowell, *Proc. Natl. Acad. Sci. U. S. A.*, 2002, **99**, 118–122.
11 S. W. Perry, J. P. Norman, J. Barbieri, E. B. Brown and H. A. Gelbard, *BioTechniques*, 2011, **50**, 98–115.
12 D. G. Nicholls, *Methods Mol. Biol.*, 2012, **810**, 119–133.
13 C. M. O'Reilly, K. E. Fogarty, R. M. Drummond, R. A. Tuft and J. V. Walsh Jr., *Biophys. J.*, 2003, **85**, 3350–3357.
14 J. Chu, R. D. Haynes, S. Y. Corbel, P. Li, E. Gonzalez-Gonzalez, J. S. Burg, N. J. Ataie, A. J. Lam, P. J. Cranfill, M. A. Baird, M. W. Davidson, H. L. Ng, K. C. Garcia, C. H. Contag, K. Shen, H. M. Blau and M. Z. Lin, *Nat. Methods*, 2014, **11**, 572–578.
15 L. S. Arakaki, D. H. Burns and M. J. Kushmerick, *Appl. Spectrosc.*, 2007, **61**, 978–985.
16 M. Monici, *Biotechnol. Annu. Rev.*, 2005, **11**, 227–256.
17 V. Magidson and A. Khodjakov, *Methods Cell Biol.*, 2013, **114**, 545–560.

18 Y. L. Huang, A. S. Walker and E. W. Miller, *J. Am. Chem. Soc.*, 2015, **137**, 10767–10776.
19 B. Chazotte, *Cold Spring Harbor Protoc.*, 2011, **2011**, 990–992.
20 L. Zhang, W. Liu, X. Huang, G. Zhang, X. Wang, Z. Wang, D. Zhang and X. Jiang, *Analyst*, 2015, **140**, 5849–5854.
21 A. Akbarzadeh, R. Rezaei-Sadabady, S. Davaran, S. W. Joo, N. Zarghami, Y. Hanifehpour, M. Samiei, M. Kouhi and K. Nejati-Koshki, *Nanoscale Res. Lett.*, 2013, **8**, 102.
22 H. W. Ai, S. G. Olenych, P. Wong, M. W. Davidson and R. E. Campbell, *BMC Biol.*, 2008, **6**, 13.
23 L. Wang, W. Li, M. Lin, M. Garcia, D. Mulholland, M. Lilly and M. Martins-Green, *Carcinogenesis*, 2014, **35**, 2321–2330.
24 R. P. Haugland, V. L. Singer and S. T. Yue, Xanthene dyes and their application as luminescence quenching compounds, *US patent number*: US6399392 B1, published on Jun 4, 2002.
25 I. D. Johnson, *The Molecular Probes Handbook: A Guide to Fluorescent Probes and Labeling Technologies*, Life Technologies Corporation, 11th edn, 2010.
26 M. Kabelac, F. Zimandl, T. Fessl, Z. Chval and F. Lankas, *Phys. Chem. Chem. Phys.*, 2010, **12**, 9677–9684.
27 A. Kholmukhamedov, J. M. Schwartz and J. J. Lemasters, *Shock*, 2013, **39**, 543.
28 C. W. Leung, Y. Hong, S. Chen, E. Zhao, J. W. Lam and B. Z. Tang, *J. Am. Chem. Soc.*, 2013, **135**, 62–65.
29 S. Hong and P. L. Pedersen, *Microbiol. Mol. Biol. Rev.*, 2008, **72**, 590–641.
30 J. P. Brennan, R. Southworth, R. A. Medina, S. M. Davidson, M. R. Duchen and M. J. Shattock, *Cardiovasc. Res.*, 2006, **72**, 313–321.
31 J. M. Li, H. Zhou, Q. Cai and G. X. Xiao, *World J. Gastroenterol.*, 2003, **9**, 562–567.